RAPID COMMUNICATIONS IN MASS SPECTROMETRY
Rapid Commun. Mass Spectrom. 2009; **23**: 2151–2160
Published online in Wiley InterScience (www.interscience.wiley.com) DOI: 10.1002/rcm.4125

RCM

Structural characterization of pregnane glycosides from *Cynanchum auriculatum* by liquid chromatography on a hybrid ion trap time-of-flight mass spectrometer

Lian-Wen Qi[1]†, Xiao-Jie Gu[1]†, Ping Li[1]*, Yan Liang[2], Haiping Hao[2] and Guangji Wang[2]*

[1]Key Laboratory of Modern Chinese Medicines, China Pharmaceutical University, Ministry of Education, Nanjing 210009, China
[2]Key Laboratory of Drug Metabolism and Pharmacokinetics, China Pharmaceutical University, Nanjing 210009, China

Received 7 January 2009; Revised 31 March 2009; Accepted 10 May 2009

A method coupling high-performance liquid chromatography with hybrid ion trap time-of-flight mass spectrometry (TOFMS) using an electrospray ionization source was firstly used to characterize ten major pregnane glycosides including one novel compound auriculoside IV from the roots of *Cynanchum auriculatum* Royle ex Wight. In the MS/MS spectra, fragmentation reactions of the $[M+Na]^+$ were recorded to provide abundant structural information on the aglycone and glycosyl moieties. Experiments using TOFMS allowed us to obtain precise elemental compositions of molecular ions and subsequent product ions with errors less than 6 ppm. The pregnane glycosides in *C. auriculatum* were classified into two major core groups: one is caudatin characterized by the neutral loss of one ikemamic acid molecule (128 Da) from the precursor ion, and the other is kidjoranin characterized by the neutral loss of cinnamic acid (148 Da) from the precursor ion. Meanwhile, a series of sugar-chain fragment ions provided valuable information about the compositions of the sugar residues and the sequences of the sugar chain. Logical fragmentation pathways for pregnane glycosides have been proposed and are useful for the identification of these compounds in natural products especially when there are no reference compounds available. Copyright © 2009 John Wiley & Sons, Ltd.

Radix Cynanchi Auriculati, derived from the roots of *Cynanchum auriculatum* Royle ex Wight belonging to Asclepiadaceae family, is a very famous herbal medicine that is widely distributed in China and India. It has been used in the clinic as a beneficial and tonic agent for more than 100 years in Traditional Chinese Medicine known as *Baishouwu*. Phytochemical and pharmacological investigations on this herb indicated that pregnane glycosides are the major bioactive constituents.[1] Pregnane glycosides are a class of pharmaceutically highly interesting natural products that have attracted much attention for their bioactivities, including antitumor, cytotoxicity, antifungal, acetylcholine esterase inhibition and antiosteoporosis.[2–6] The availability of effective methods for the structural characterization and identification of pregnane glycosides is of significant importance. Due to their structural complexity, high polarity, thermal lability and low abundance in plants, it is difficult to analyze pregnane glycosides by traditional strategies that involve extraction, isolation, purification and identification by chemical manipulations and spectroscopic methods. Although nuclear magnetic resonance (NMR) is the most efficient method for complete structural elucidation of chemical compounds, a relatively large amount of purified sample is required and the isolation procedure from a complicated mixture is very time-consuming and costly. Hence it is desirable to develop rapid and sensitive methods for the structural characterization of pregnane glycosides in *C. auriculatum*.

The coupling of high-performance liquid chromatography (HPLC) and electrospray ionization mass spectrometry (ESI-MS) combines the efficient separation capability of HPLC and the great power of structural characterization of MS. It provides a powerful approach to characterize and identify a variety of polar and thermally labile compounds such as pregnane glycosides in crude extracts of plants.[7–14] Various hyphenated and hybrid mass spectrometers have now been widely adopted, and, among them, time-of-flight (TOF)MS and its hybrid or in combination use with tandem mass spectrometry (MS/MS) has proven to be very powerful tools for the structural characterization of natural compounds in view of their complementary capacity to provide multistage fragmentations and accurate mass measurements for precise elemental compositions of molecular ions and subsequent product ions. Recently, the combination use of LC/ion trap multistage mass spectrometry (IT-MS^n) and LC/TOF-MS has been successfully applied to the identification and characterization of target compounds in various fields.[15–18]

So far, there has been no systematic study for the complete characterization and fragmentation mechanisms of pregnane glycosides in *C. auriculatum* by ESI-MS/MS. Herein is described an extensive investigation on the fragmentation

**Correspondence to*: P. Li or G. Wang, China Pharmaceutical University, No. 24 Tonejia Lane, Nanjing 210009, China.
E-mail: liping2004@126.com; guangjiwang@hotmail.com
†These authors contributed equally to this work.
Contract/grant sponsor: The National Science Foundation and National Key Technologies R&D Program of China; contract/grant number: 30530870.

pathways of ten pregnane glycosides including one novel compound. Fragmentation rules and key diagnostic fragment ions for these compounds have been summarized, and possible pathways of fragmentation have been proposed. Some useful characteristic fragmentation information such as the sugar composition and sequence of the carbohydrate portion has also been obtained, providing simple and rapid methods for the identification of this class of compounds.

EXPERIMENTAL

Reagents and materials

Acetonitrile and methanol (HPLC grade) were purchased from Merck (Darmstadt, Germany). Formic acid (purity 96%) was purchased from Tedia (Fairfield, OH, USA). Deionized water (18 MΩ) was prepared by passing distilled water through a Milli-Q system (Millipore, Milford, MA, USA). Other reagents and chemicals were of analytical grade.

The roots of *C. auriculatum* were collected from Jiangsu Province of China, and authenticated by Dr. Ping Li, Professor of the Department of Pharmacognosy, China Pharmaceutical University, Nanjing, China. Voucher specimens (No.WFC-2004525-3) were deposited in the herbarium of the Key Laboratory of Modern Chinese Medicines, Ministry of Education, Department of Pharmacognosy, China Pharmaceutical University.

Extraction and isolation of reference compounds

The dried powders of the roots of *C. auriculatum* (1 kg) were extracted three times with 95% ethanol under reflux for 2 h each time, and the ethanol was evaporated under reduced pressure. The extraction was suspended in 500 mL water, and then partitioned with the same volume of petroleum ether, chloroform and *n*-butanol, respectively. The chloroform fraction was submitted to column chromatography on silica gel (750 g) with a gradient elution of chloroform/methanol (98:2, 95:5, 85:15, v/v) to give three fractions (I–III) and the *n*-butanol fraction was chromatographed on a silica gel column (500 g) with chloroform/methanol (15:1, 10:1, 4:1, v/v) as elution to give another three fractions (IV–VI). Fractions II, III and VI were finally purified by semi-preparative HPLC on a Waters 600E HPLC system equipped with a 2487 UV detector set at 220 nm (Waters Co., Milford, MA, USA) with a methanol/water solvent system to afford ten major pregnane glycosides named Pg1–Pg10.

Semi-preparative HPLC on a Waters 600E HPLC system equipped with a Waters 2487 dual-wavelength UV detector was used to prepare one new pregnane glycoside Pg-1. The semi-preparative separation was achieved on a reversed-phase Zorbax RX-C_{18} column (9.4 mm × 250 mm, 5 μm); the column temperature was maintained at room temperature. The mobile phase was acetonitrile/water (40:60, v/v). The flow rate was 2.5 mL/min and the UV detection wavelength was 220 nm. The structures of the ten pregnane glycosides (shown in Fig. 1) were elucidated by spectroscopic methods including extensive 1D- and 2D-NMR experiments, and compared with literature publications.[19–22] 1D- and 2D-NMR spectra were recorded on a Bruker AV-500 spectrometer (^{1}H 500 MHz, ^{13}C 125 MHz), using pyridine (C_5D_5N) as a solvent and TMS as internal standard.

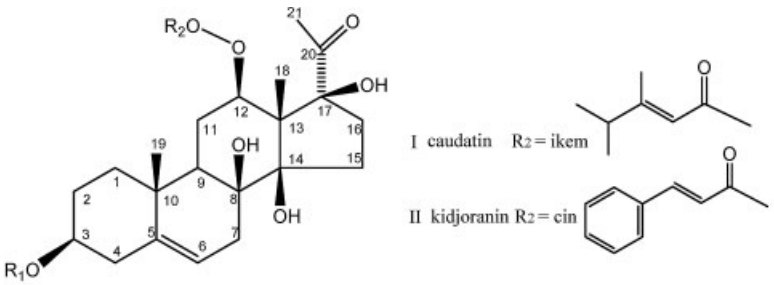

Pg	Name	R_2	[a]R_1
1	auriculoside IV	II	β-D-Glc-β-D-Glc-α-L-Cym-β-D-Cym-α-L-Dig-β-D-Cym-
2	cynauricuoside C	I	β-D-Glc-β-D-Glc-α-L-Cym-β-D-Cym-α-L-Dig-β-D-Cym-
3	cynauricuoside A	II	β-D-Glc-α-L-Cym-β-D-Cym-α-L-Dig-β-D-Cym-
4	wilfoside C1G	I	β-D-Glc-α-L-Cym-β-D-Cym-α-L-Dig-β-D-Cym-
5	cynanauriculoside I	II	β-D-Glc-α-L-Cym-β-D-Cym-α-L-Cym-β-D-Dit-α-L-Cym-β-D-Dit-
6	cynanauriculoside II	II	β-D-Glc-α-L-Cym-β-D-Cym-α-L-Cym-β-D-Cym-α-L-Cym-β-D-Dit-
7	caudatin3-*O*-β-cym	I	β-D-Cym-
8	wilfoside K1N	II	α-L-Cym-β-D-Cym-α-L-Dig-β-D-Cym-
9	wilfoside C3N	I	β-D-Cym-α-L-Dig-β-D-Cym-
10	wilfoside C1N	I	α-L-Cym-β-D-Cym-α-L-Dig-β-D-Cym-

[a] In all compounds sugar chain was linked linear to the C-3 hydroxyl group of the aglycone. Cym: cymaropyranosyl, Dig: diginopyranosyl, Dit: digitoxopyranosyl, Glc: glucopyranosyl, Cin: cinnamoyl, Ikem: ikemamoyl. The linkage mode of the saccharide was 1→4.

Figure 1. Structures of ten pregnane glycosides found in the roots of *C. auriculatum*.

DOI: 10.1002/rcm

Sample preparation

The crude powder of roots was extracted three times with 95% ethanol under reflux for 2 h each time, and ethanol was evaporated under reduced pressure. Then the extract was subjected to a silica gel column eluting with chloroform/methanol in the ratio of 50:1 and 4:1 (v/v) to give fractions I and II. Fraction II, as the pregnane glycoside fraction, was dissolved in methanol, filtered through a 0.45 μm microporous membrane and stored at 4°C until analysis.

Apparatus, chromatographic and MS conditions

HPLC analyses were performed on a Shimadzu analytical HPLC instrument (Kyoto, Japan) coupled to a LC-20AD pump, CTO-20AC column oven, DGU-20A degasser, and SIL-20AC autoinjector. The separation was carried out on a Phenomenex C_{18} column (4.6 mm × 250 mm, 5.0 μm) with the column temperature at 25°C. The mobile phase consisted of water (A) and acetonitrile (B) using a gradient elution of 49% B at 0–15 min, 49–62% B at 15–18 min, 62% B at 18–23 min, and 62–85% B at 23–33 min. The mobile phase was split into two identical parts with 0.4 mL/min flowing into the MS detector. The detection wavelength was set at 220 nm.

The IT-TOFMS system consisted of a Shimadzu hybrid IT-TOF mass spectrometer with an ESI source. Mass spectrometer conditions were optimized to obtain maximal sensitivity. Positive ion mode was used to provide sensitive signals and abundant fragment ions. The curve dissolution line (CDL) temperature and the block heater temperature were maintained at 200°C. The capillary voltage, CDL voltage and detector voltage were fixed at 4.5 kV, −10 V and 1.6 kV, respectively. Nitrogen was used as the nebulizer gas at a flow rate of 1.5 L/min. Mass spectra were obtained over the range *m/z* 300–1800. In the automatic mode, all ions were first accumulated in the octopole and then rapidly pulsed into the ion trap for MS^n analyses according to the criteria settings. All ions produced were finally introduced into the TOF instrument for accurate mass determination. The ion accumulation time was 10 ms. To increase mass accuracy, the TOF mass spectrometer was calibrated routinely in the positive ESI mode using a lock-mass trifluoroacetic acid sodium solution. The entire mass range from *m/z* 100 to 3000 was calibrated with this lock-mass solution. The infusion of this solution was performed every day for an accurate calibration of the TOF analyzer. Experiments using TOFMS showed accurate mass measurements of molecular ions in MS spectra and subsequent product ions in MS/MS spectra were obtained for the ten analytes with errors less than 6 ppm, demonstrating a high validation of this calibration method. The data acquisition and processing were performed by the LC/MS solution version 3.4 software (Shimadzu, Tokyo, Japan), including a formula predictor to predict chemical formulas.

RESULTS AND DISCUSSION

Nomenclature

As shown in Fig. 1, a pregnane glycoside generally consists of a pregnane aglycone skeleton and a single oligosaccharide chain at *C*-3. Based on the structural difference in the acyl group at *C*-12, the ten pregnane glycosides could be divided into two groups, one with a caudatin skeleton including Pg-2, 4, 7, 9 and 10, and the other with a kidjoranin skeleton including Pg-1, 3, 5, 6 and 8. The oligosaccharide moiety contains one to seven 2,6-dideoxyhexopyranoses (cymaropyranose and/or diginopyranose and/or digitoxopyranose) and/or hexopyranoses (glucopyranoses). The linkage mode among all saccharides was 1→4 for the ten pregnane glycosides. The nomenclature system suggested by Domon and Costello for the cleavage of the carbohydrate part was adopted to denote the glycoside fragment ions.[23] The ions containing the charge at the reducing terminus are termed Y_j, where j is the number of the interglycosidic bond broken, counting from the aglycone, and the glycosidic bond linking the glycosyl part to the aglycone is numbered 0, whereas those ions retaining the charge on the carbohydrate residue are designated as C_i, B_i and $^{k,l}A_i$, where i represents the number of the glycosidic bond cleaved counting from the non-reducing terminus, and the superscripts k and l indicate the cleavage site within the carbohydrate rings.

Because of the ubiquitous presence of sodium ions during the ionization of the glycosides, and the strong affinity of sugars for sodium ions, the $[M+Na]^+$ ions were dominant in the positive mass spectra of all pregnane glycosides and are discussed here with respect to their full-scan MS and MS^n data. Structures were characterized based on the fragmentation reactions of the $[M+Na]^+$ ions and are presented in the following sections. Because of the instability of the sugar chain, all of the fragment ions were obtained from the precursor ion $[M+Na]^+$ in MS^2; no product ions were observed in the MS^3 spectrum.

Structural characterization of Pg-1 and Pg-2

As shown in Fig. 2(a), Pg-2 generated a molecular ion peak with great intensity at *m/z* 1413.7078 for $[M+Na]^+$ in positive ion mode, which corresponded to the molecular formula of $C_{68}H_{110}O_{29}$. As can be seen from the MS^2 spectrum in Fig. 2(b), the precursor $[M+Na]^+$ ion produced abundant fragment ions, and the precursor ions $[M+Na]^+$ were not observed in its MS/MS spectrum, which might result from extensive fragmentation of the precursor ion. One characteristic product ion $[M+Na\text{-ikem}]^+$ at *m/z* 1285.6260 was formed by a diagnostic loss of 128 Da corresponding to the neutral elimination of one molecule of ikemamic acid at *C*-12. The first Y series of product ions were characterized by the involution of the aglycone moiety. Y_5 at *m/z* 1123.5628, Y_4 at 961.5152 and Y_3 at 817.4336 were produced by successive losses of the terminal glucopyranose unit (162 Da), the intermediate glucopyranose unit and the subsequent cymaropyranose unit (144 Da) from $[M+Na\text{-ikem}]^+$, respectively. The second series were characterized by sugar-chain fragment ions, providing valuable information for sugar compositions and their linkage sequences. The pentasaccharide ion C_6-B_1 at *m/z* 779.3250 was formed by cleavage of the aglycone with retention of the glycosidic oxygen atom and additional loss of the terminal glucopyranose unit. Loss of the reducing end cymaropyranose residue (144 Da) from the C_6-B_1 ion produced a high abundance tetrasaccharide ion C_5-B_1 at *m/z* 635.2537, and consecutive loss of one diginopyranose residue (144 Da) from C_5-B_1 generated a

DOI: 10.1002/rcm

RCM

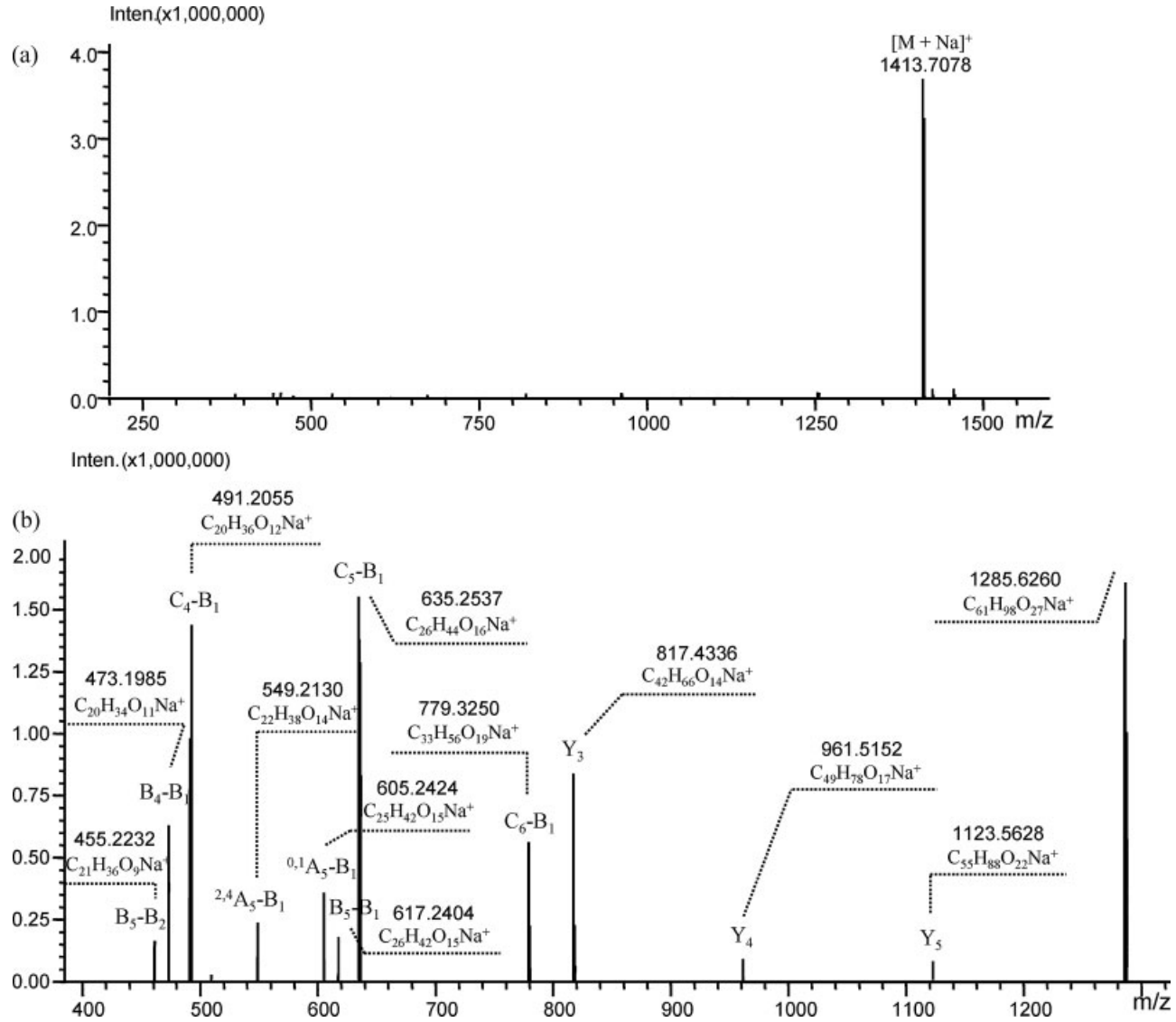

Figure 2. Positive ion ESI-MS spectrum (a) and MS^2 spectrum (b) of $[M+Na]^+$ for Pg-2.

trisaccharide ion C_4-B_1 at *m/z* 491.2055. The fragment ions at *m/z* 617.2404 and 473.1985 were assigned as B_5-B_1 and B_4-B_1 also by glycosidic bond cleavage but without the glycosidic oxygen atom compared with 635.2537 and 491.2055. The fragment ion B_5-B_2 at *m/z* 455.2232 was produced by the loss of another glucopyranose unit (162 Da) from B_5-B_1. Besides, cross-ring cleavage ions of $^{2,4}A_5$-B_1 at *m/z* 549.2130 and $^{0,1}A_5$-B_1 at *m/z* 605.2424 were produced from 2,4- and 0,1-bond cleavages of the diginopyranose unit. The MS^2 data of the $[M+Na]^+$ ion of Pg-2 as well as corresponding elemental compositions and ppm errors are listed in Table 1. Accurate mass measurements within 6 ppm error were achieved for the molecular ion and subsequent fragment ions. The fragmentation pathways are proposed in Scheme 1.

Pg-1, a novel compound isolated from *C. auriculatum* by the authors,[24] produced a molecular ion peak at *m/z* 1433.6759 for $[M+Na]^+$ corresponding to the molecular formula of $C_{70}H_{106}O_{29}$. The MS^2 spectral data from the precursor $[M+Na]^+$ ion are also summarized in Table 1. As seen from Table 1, Pg-1 generated the same fragment ions as those of Pg-2, demonstrating Pg-1 has the same skeleton and oligosaccharide chain as Pg-2. The only differences between Pg-1 and Pg-2 in mass spectra were that the characteristic product ion at *m/z* 1285.6196 was formed by a loss of 148 Da corresponding to the diagnostic neutral loss of one molecule of cinnamic acid, rather than 128 Da representing the loss of one molecule of ikemamic acid from the precursor ion.

Structural characterization of Pg-3 and Pg-4

Pg-3 and Pg-4 yielded intensive molecular ion peaks at *m/z* 1271.6240 and 1251.6507 for $[M+Na]^+$, which corresponded to the molecular formulas of $C_{64}H_{96}O_{24}$ and $C_{62}H_{100}O_{24}$ with errors of 4.40 and 0.80 ppm, respectively. Table 2 shows the accurate mass measurements of major fragment ions observed in MS^2 spectra of $[M+Na]^+$ precursor ions for Pg-3 and Pg-4. Pg-3 and Pg-4 generated the same fragment ions, indicating that they have similar skeletons and oligosaccharide chains. The characteristic product ion at *m/z* 1123.57 was formed by the neutral loss of cinnamic acid (148 Da) from the precursor ion 1271.6240 for Pg-3, while the neutral loss of ikemamic acid (128 Da) from 1251.6507 was

DOI: 10.1002/rcm

Table 1. Accurate mass measurements of major fragment ions observed in MS^2 spectra of $[M+Na]^+$ precursor ions for Pg-1 and Pg-2

	Pg-1				Pg-2			
Fragments	Elem. comp.	Measured *m/z*	Calculated *m/z*	Error (ppm)	Elem. comp.	Measured *m/z*	Calculated *m/z*	Error (ppm)
$[M+Na]^+$	$C_{70}H_{106}O_{29}Na^+$	1433.6759	1433.6712	3.28	$C_{68}H_{110}O_{29}Na^+$	1413.7078	1413.7025	3.75
$[M+Na\text{-ikem}]^+$	—	—	—	—	$C_{61}H_{98}O_{27}Na^+$	1285.6260	1285.6188	5.60
$[M+Na\text{-cin}]^+$	$C_{61}H_{98}O_{27}Na^+$	1285.6196	1285.6188	0.62	—	—	—	—
Y_5	$C_{55}H_{88}O_{22}Na^+$	1123.5659	1123.5659	0.00	$C_{55}H_{88}O_{22}Na^+$	1123.5628	1123.5659	−3.42
Y_4	$C_{49}H_{78}O_{17}Na^+$	961.5115	961.5131	−1.90	$C_{49}H_{78}O_{17}Na^+$	961.5152	961.5131	2.28
Y_3	$C_{42}H_{66}O_{14}Na^+$	817.4340	817.4345	−0.61	$C_{42}H_{66}O_{14}Na^+$	817.4336	817.4345	−1.40
C_6-B_1	$C_{33}H_{56}O_{19}Na^+$	779.3317	779.3308	1.15	$C_{33}H_{56}O_{19}Na^+$	779.3250	779.3308	−5.13
C_5-B_1	$C_{26}H_{44}O_{16}Na^+$	635.2501	635.2522	−3.31	$C_{26}H_{44}O_{16}Na^+$	635.2537	635.2522	2.36
C_4-B_1	$C_{20}H_{36}O_{12}Na^+$	491.2071	491.2099	−3.94	$C_{20}H_{36}O_{12}Na^+$	491.2055	491.2099	−4.80
B_5-B_1	$C_{26}H_{42}O_{15}Na^+$	617.2439	617.2416	3.62	$C_{26}H_{42}O_{15}Na^+$	617.2404	617.2416	−2.07
B_4-B_1	$C_{20}H_{34}O_{11}Na^+$	473.1969	473.1993	−4.07	$C_{20}H_{34}O_{11}Na^+$	473.1985	473.1993	−1.69
B_5-B_2	$C_{21}H_{36}O_9Na^+$	455.2140	455.2252	−1.46	$C_{21}H_{36}O_9Na^+$	455.2232	455.2252	−2.16
$^{0,1}A_5$-B_1	$C_{25}H_{42}O_{15}Na^+$	605.2412	605.2416	−0.49	$C_{25}H_{42}O_{15}Na^+$	605.2424	605.2416	1.32
$^{2,4}A_5$-B_1	$C_{22}H_{38}O_{14}Na^+$	549.2177	549.2154	3.60	$C_{22}H_{38}O_{14}Na^+$	549.2130	549.2154	−2.60

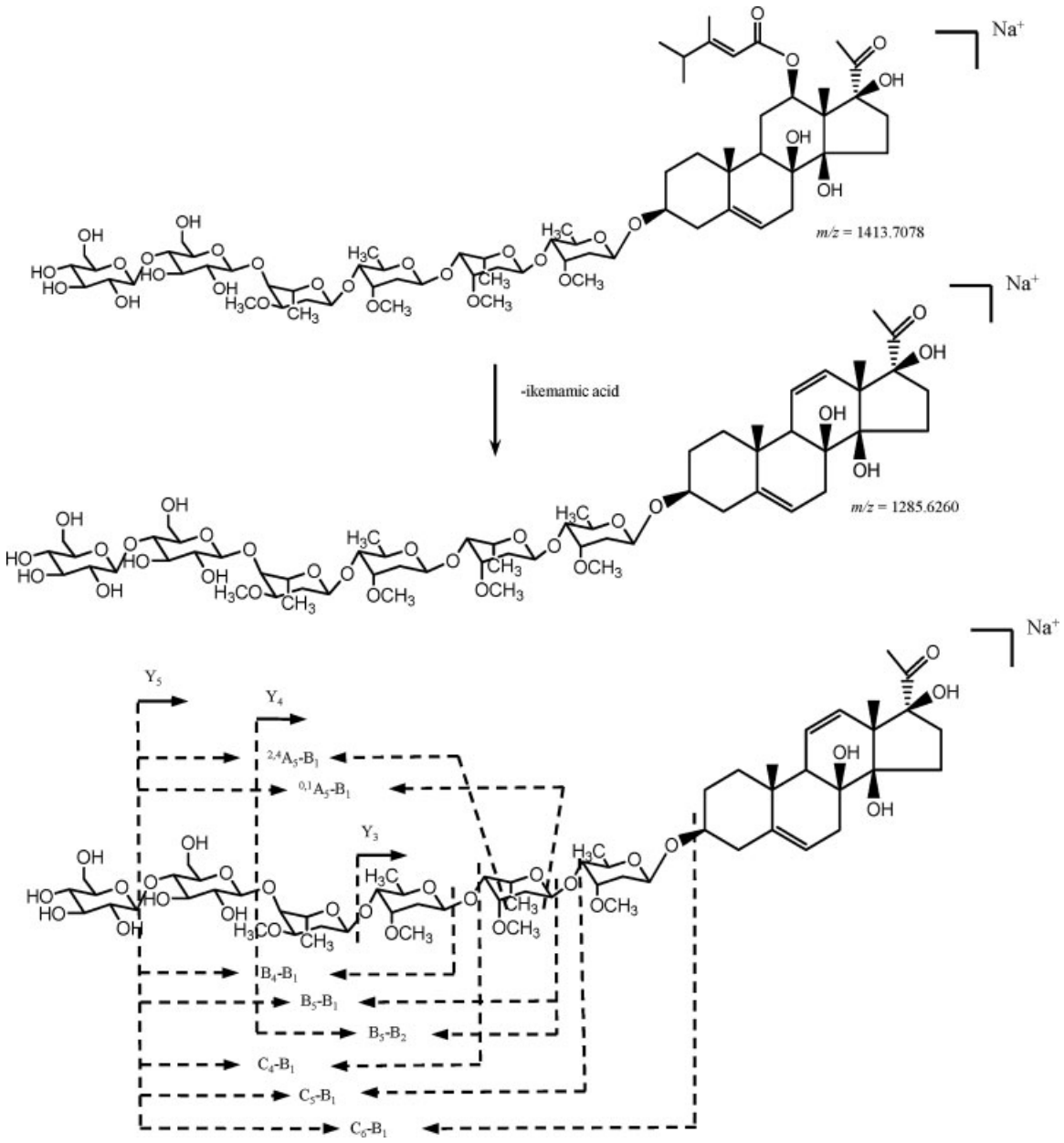

Scheme 1. Fragmentation pathway proposed for $[M+Na]^+$ ions of Pg-2.

DOI: 10.1002/rcm

RCM

Table 2. Accurate mass measurements of major fragment ions observed in MS^2 spectra of $[M+Na]^+$ precursor ions for Pg-3 and Pg-4

	Pg-3				Pg-4			
Fragments	Elem. comp.	Measured *m/z*	Calculated *m/z*	Error (ppm)	Elem. comp.	Measured *m/z*	Calculated *m/z*	Error (ppm)
$[M+Na]^+$	$C_{64}H_{96}O_{24}Na^+$	1271.6240	1271.6184	4.40	$C_{62}H_{100}O_{24}Na^+$	1251.6507	1251.6497	0.80
$[M+Na\text{-ikem}]^+$	—	—	—	—	$C_{55}H_{88}O_{22}Na^+$	1123.5670	1123.5659	1.00
$[M+Na\text{-cin}]^+$	$C_{55}H_{88}O_{22}Na^+$	1123.5697	1123.5659	3.46	—	—	—	—
Y_4	$C_{49}H_{78}O_{17}Na^+$	961.5140	961.5131	0.94	$C_{49}H_{78}O_{17}Na^+$	961.5169	961.5131	3.95
Y_3	$C_{42}H_{66}O_{14}Na^+$	817.4375	817.4345	3.67	$C_{42}H_{66}O_{14}Na^+$	817.4389	817.4345	5.38
B_4	$C_{26}H_{42}O_{15}Na^+$	617.2449	617.2416	3.78	$C_{26}H_{42}O_{15}Na^+$	617.2413	617.2416	−0.46
B_3	$C_{20}H_{34}O_{11}Na^+$	473.1995	473.1993	0.42	$C_{20}H_{34}O_{11}Na^+$	473.2010	473.1993	3.59

observed for Pg-4, which demonstrated that Pg-3 has a kidjoranin skeleton while Pg-4 has a caudatin skeleton.

The Y_4 ion at *m/z* 961.51 and the Y_3 ion at 817.43 for Pg-3 or Pg-4 were produced by loss of the terminal glucopyranose unit (162 Da), and successive loss of the subsequent glucopyranose unit and the subsequent cymaropyranose unit (144 Da) from $[M+Na\text{-ikem/cin}]^+$. The B_4 ion at *m/z* 617.24 was formed by losses of the aglycone and the reducing end cymaropyranose unit, while the B_3 ion at *m/z* 473.20 was generated through consecutive loss of the diginopyranose unit (144 Da) from B_4. It can be seen from Tables 1 and 2 that the molecular weight of Pg-3 (or Pg-4) is 162 Da less than that of Pg-1 (or Pg-2), corresponding to one glucopyranose unit, and the product ions of Pg-3 (or Pg-4) at *m/z* 961.51, 817.44, 617.24 and 473.20 were identical to the Y_4, Y_3, B_5-B_1 and B_4-B_1 ions of Pg-1 (or Pg-2), indicating they have similar sugar compositions and linkage sequences to some extent except for the absence of the terminal glucopyranose unit for Pg-3 and Pg-4.

Structural characterization of Pg-5 and Pg-6

As shown in Fig. 3(a), Pg-5 produced a high abundance $[M+Na]^+$ ion at *m/z* 1531.7473 corresponding to the

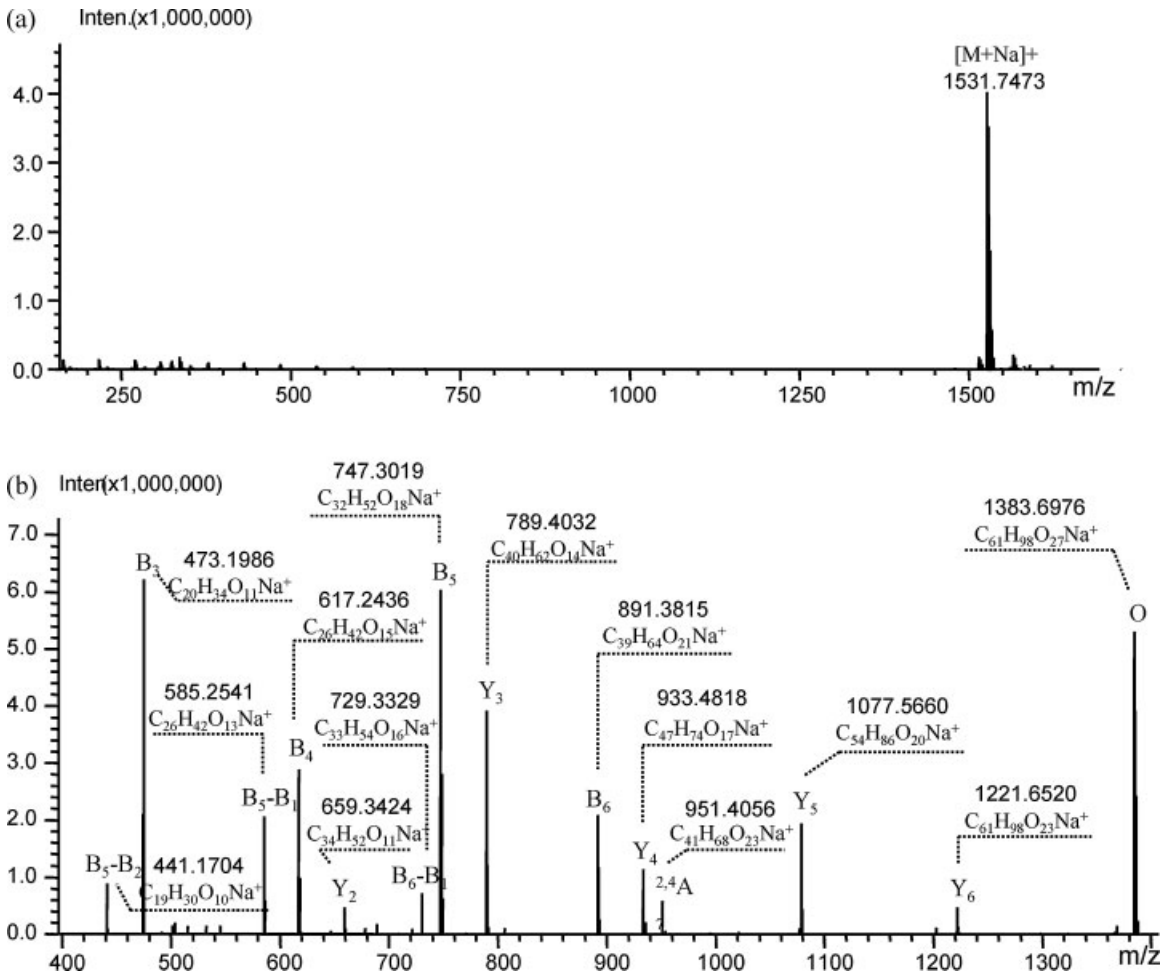

Figure 3. Positive ion ESI-MS spectrum (a) and MS^2 spectrum (b) of $[M+Na]^+$ for Pg-5. 'O' refers to the $[M+Na\text{-cin}]^+$ ion.

DOI: 10.1002/rcm

elemental composition of $C_{76}H_{116}O_{30}Na^+$ with an error of 2.28 ppm. In the MS^2 spectrum of the precursor $[M+Na]^+$ ion shown in Fig. 3(b), diagnostic neutral loss of one cinnamic acid molecule (148 Da) from the $[M+Na]^+$ ion yielded a characteristic fragment ion $[M+Na\text{-cin}]^+$ at *m/z* 1383.6976. The Y series of ions included Y_6, Y_5, Y_4, Y_3 and Y_2 ions at *m/z* 1221.6520, 1077.5660, 933.4818, 789.4032 and 659.3424 by successive losses of the terminal glucopyranose residue (162 Da), the subsequent cymaropyranose residue (144 Da), the consecutive cymaropyranose residue (144 Da), the next cymaropyranose residue (144 Da) and the digitoxopyranose residue (130 Da) from $[M+Na\text{-cin}]^+$. The successive losses of one reducing end digitoxopyranose moiety (130 Da), one internal cymaropyranose moiety (144 Da), one intermediate digitoxopyranose (130 Da) unit and the following cymaropyranose moiety from the whole sugar chain generated predominant B_6, B_5, B_4 and B_3 ions, located at *m/z* 891.3815, 747.3019, 617.2436 and 473.1986, respectively. The fragments B_6-B_1 at *m/z* 729.3329 and B_5-B_1 at *m/z* 585.2541 were formed by further elimination of the terminal glucopyranose unit from the B_6 and B_5 ions, respectively. The B_5-B_2 ion at *m/z* 441.1704 was produced by additional loss of an additional cymaropyranose unit from B_5-B_1. The characteristic presence of the cross-ring cleavage ion $^{2,4}A_7$ at *m/z* 951.4056 was produced from 2,4-bond cleavage of the reducing terminal digitoxopyranose residue. The MS^2 data of the $[M+Na]^+$ ion of Pg-2 as well as corresponding elemental compositions and ppm errors are listed in Table 3. Accurate mass measurements within 6 ppm error were achieved for the molecular ion and subsequent fragment ions. The fragmentation pathways are proposed in Scheme 2(a).

The accurate mass value of the $[M+Na]^+$ ion corresponding to Pg-6 was 1545.7661 consistent with an elemental composition of $C_{77}H_{118}O_{30}Na^+$ with an error of 3.88 ppm. The MS^2 spectral data from the precursor ion of 1545.7661 are also summarized in Table 3. The $[M+Na\text{-cin}]^+$ ion at *m/z* 1397.7158 was found in its MS^2 spectrum by the neutral loss of one cinnamic acid molecule (148 Da). Most of the Y, B and A series of fragment ions of Pg-6 were 14 Da larger than those of Pg-5, predicting that the glycosyl moiety of Pg-6 had one more CH_2 group. The same fragment ions, Y_2 at *m/z* 659.34, B_4 at *m/z* 617.24 and B_3 at *m/z* 473.20, indicated that the third monosaccharide unit for Pg-6 was different from Pg-5. The mass difference between fragment ions B_5 and B_4 was 144 Da, which indicated the third monosaccharide unit for Pg-6 was a cymaropyranose unit instead of a digitoxopyranose unit for Pg-5. The ions $^{2,4}A_7$ at *m/z* 965.4232, $^{3,5}A_5$ at *m/z* 675.2820 and $^{3,5}A_4$ at *m/z* 531.2021 were produced from 2,4-bond cleavages of the reducing end digitoxopyranose, 3,5-bond cleavages of the third and the fourth cymaropyranose. The fragmentation pathways are proposed in Scheme 2(b).

Structural characterization of Pg-7, 8, 9 and 10

Pg-7, 8, 9 and 10 produced abundant $[M+Na]^+$ peaks at *m/z* 657.3633, 1109.5687, 945.5227 and 1089.6016, corresponding to the formulas $C_{35}H_{54}O_{10}Na^+$, $C_{58}H_{86}O_{19}Na^+$, $C_{49}H_{78}O_{16}Na^+$ and $C_{56}H_{90}O_{19}Na^+$, respectively, with ppm errors less than 5. Table 4 shows the accurate mass measurements of major fragment ions observed in MS^2 spectra of $[M+Na]^+$ precursor ions for these four compounds. Pg-7, 9 and 10 could be rapidly assigned as the caudatin skeleton type characterized by the neutral loss of one ikemamic acid molecule (128 Da), while Pg-8 belonged to the kidjoranin skeleton type characterized by the neutral loss of one cinnamic acid molecule (148 Da). The MS^2 spectrum of Pg-7 did not produce other product ions except for a high abundance $[M+Na\text{-ikem}]^+$ peak. For Pg-9, successive losses of the terminal cymaropyranose residue (144 Da) and the subsequent digitoxopyranose residue (130 Da) from the $[M+Na\text{-ikem}]^+$ ion produced the product ions Y_2 at *m/z* 673.3558 and Y_1 at 529.2749. The whole sugar-chain fragment ion B_3 at *m/z* 455.2232 was observed and produced by cleavage of the glycosidic bond between the aglycone and the reducing end of the sugar chain. Successive loss of the following

Table 3. Accurate mass measurements of major fragment ions observed in MS^2 spectra of $[M+Na]^+$ precursor ions for Pg-5 and Pg-6

	Pg-5				Pg-6			
Fragments	Elem. comp.	Measured *m/z*	Calculated *m/z*	Error (ppm)	Elem. comp.	Measured *m/z*	Calculated *m/z*	Error (ppm)
$[M+Na]^+$	$C_{76}H_{116}O_{30}Na^+$	1531.7479	1531.7444	2.28	$C_{77}H_{118}O_{30}Na^+$	1545.7661	1545.7600	3.88
$[M+Na\text{-cin}]^+$	$C_{67}H_{108}O_{28}Na^+$	1383.6976	1383.6919	4.12	$C_{68}H_{110}O_{28}Na^+$	1397.7158	1397.7076	5.87
Y_6	$C_{61}H_{98}O_{23}Na^+$	1221.6520	1221.6568	−3.20	$C_{62}H_{100}O_{23}Na^+$	1235.6494	1235.6548	−4.37
Y_5	$C_{54}H_{86}O_{20}Na^+$	1077.5660	1077.5605	5.10	$C_{55}H_{88}O_{20}Na^+$	1091.5791	1097.5761	2.75
Y_4	$C_{47}H_{74}O_{17}Na^+$	933.4818	933.4818	0.00	$C_{48}H_{76}O_{17}Na^+$	947.4979	947.4975	0.42
Y_3	$C_{40}H_{62}O_{14}Na^+$	789.4032	789.4032	0.00	$C_{41}H_{64}O_{14}Na^+$	803.4199	803.4188	1.37
Y_2	$C_{34}H_{52}O_{11}Na^+$	659.3424	659.3402	2.63	$C_{34}H_{52}O_{11}Na^+$	659.3368	659.3402	−5.16
B_6	$C_{39}H_{64}O_{21}Na^+$	891.3815	891.3832	−1.90	$C_{40}H_{66}O_{21}Na^+$	905.3977	905.3989	−1.25
B_5	$C_{32}H_{52}O_{18}Na^+$	747.3019	747.3046	−3.60	$C_{33}H_{54}O_{18}Na^+$	761.3203	761.3202	0.12
B_4	$C_{26}H_{42}O_{15}Na^+$	617.2436	617.2416	3.24	$C_{26}H_{42}O_{15}Na^+$	617.2400	617.2416	−2.58
B_3	$C_{20}H_{34}O_{11}Na^+$	473.1986	473.1993	−1.48	$C_{20}H_{34}O_{11}Na^+$	473.2003	473.1993	2.11
B_6-B_1	$C_{33}H_{54}O_{16}Na^+$	729.3329	729.3304	3.43	—	—	—	—
B_5-B_1	$C_{26}H_{42}O_{13}Na^+$	585.2541	585.2518	3.93	$C_{27}H_{44}O_{13}Na^+$	599.2652	599.2674	−3.67
B_5-B_2	$C_{19}H_{30}O_{10}Na^+$	441.1704	441.1731	−5.69	$C_{20}H_{32}O_{10}Na^+$	455.1866	455.1888	−4.84
$^{2,4}A_7$	$C_{41}H_{68}O_{23}Na^+$	951.4056	951.4044	1.26	$C_{42}H_{70}O_{23}Na^+$	965.4232	965.4200	3.31
$^{3,5}A_5$	—	—	—	—	$C_{29}H_{48}O_{16}Na^+$	675.2820	675.2835	−2.22
$^{3,5}A_4$	—	—	—	—	$C_{22}H_{36}O_{13}Na^+$	531.2021	531.2048	−5.07

DOI: 10.1002/rcm

RCM

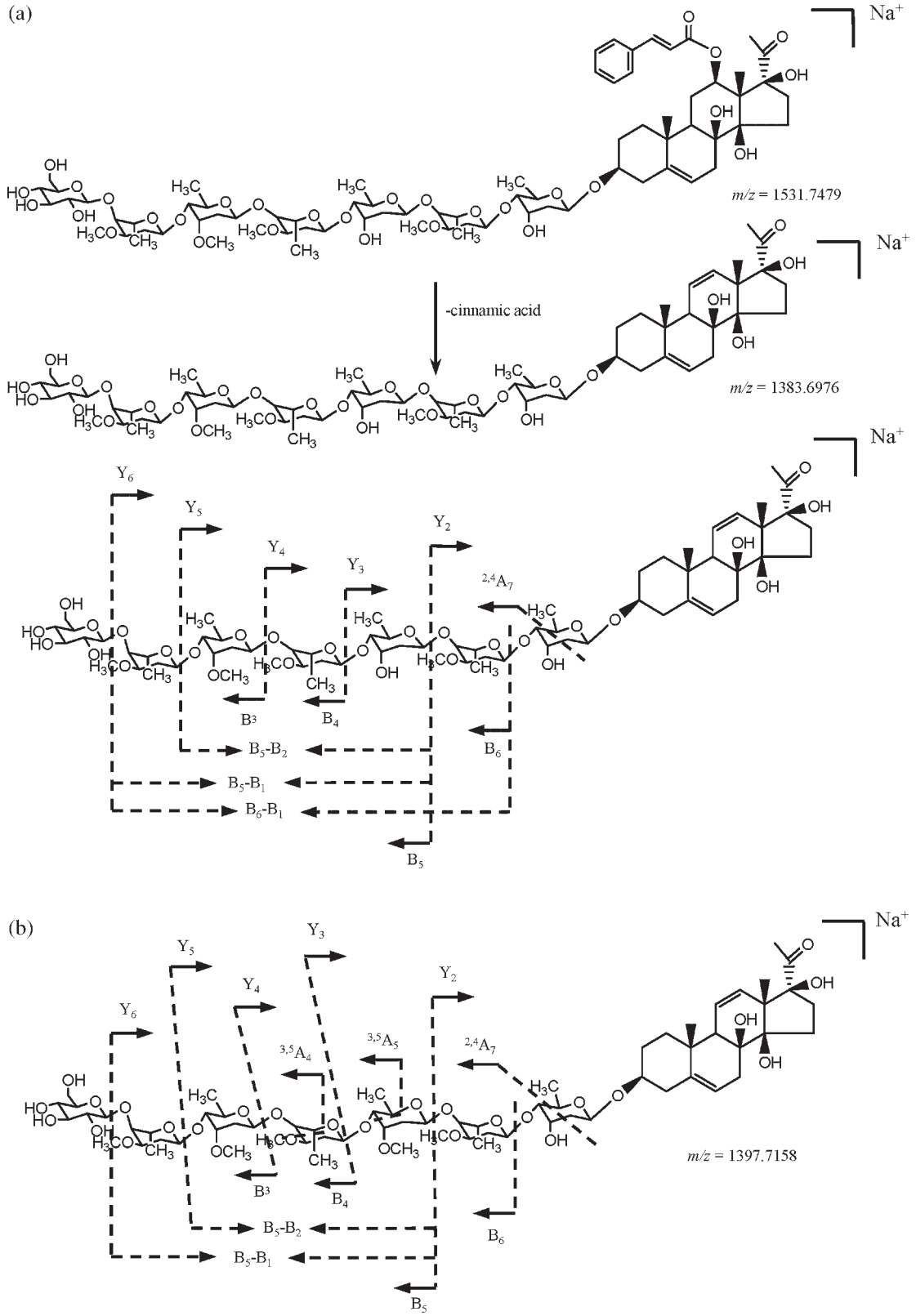

Scheme 2. Fragmentation pathways proposed for $[M+Na]^+$ ions of Pg-5 (a) and Pg-6 (b).

reducing end cymaropyranose unit (144 Da) generated a B_3 ion at *m/z* 311.1419.

Pg-8 and 10 generated similar sugar fragment ions, indicating that they have the same similar oligosaccharide chain. Successive losses of the terminal cymaropyranose residue (144 Da) and cymaropyranose residue (144 Da) from the $[M+Na\text{-ikem/cin}]^+$ ion formed the product ions Y_3 at *m/z* 817.4359 and Y_2 at 673.3570. The B_3 ion at *m/z* 455.2239 and the B_2 ion at 311.1449 were also observed for Pg-8 and 10, which were identical to those of Pg-9, demonstrating the same composition and sequence of the three terminal sugar units of Pg-8, 9 and 10.

DOI: 10.1002/rcm

Table 4. Accurate mass measurements of major fragment ions observed in MS^2 spectra of $[M+Na]^+$ precursor ions for Pg-7, 8, 9, and 10

	Pg-7				Pg-9			
Fragments	Elem. comp.	Measured *m/z*	Calculated *m/z*	Error (ppm)	Elem. comp.	Measured *m/z*	Calculated *m/z*	Error (ppm)
$[M+Na]^+$	$C_{35}H_{54}O_{10}Na^+$	657.3633	657.3621	1.82	$C_{49}H_{78}O_{16}Na^+$	945.5227	945.5182	4.76
$[M+Na\text{-ikem}]^+$	$C_{28}H_{42}O_8Na^+$	529.2778	529.2772	1.13	$C_{42}H_{66}O_{14}Na^+$	817.4351	817.4345	0.73
Y_2	—	—	—	—	$C_{35}H_{54}O_{11}Na^+$	673.3558	673.3558	−0.00
Y_1	—	—	—	—	$C_{28}H_{42}O_8Na^+$	529.2749	529.2772	−4.13
B_3	—	—	—	—	$C_{21}H_{36}O_9Na^+$	455.2232	455.2252	−3.98
B_2	—	—	—	—	$C_{14}H_{24}O_6Na^+$	311.1449	311.1465	−4.14
	Pg-8				Pg-10			
Fragments	Elem. comp.	Measured *m/z*	Calculated *m/z*	Error (ppm)	Elem. comp.	Measured *m/z*	Calculated *m/z*	Error (ppm)
$[M+Na]^+$	$C_{58}H_{86}O_{19}Na^+$	1109.5687	1109.5656	2.79	$C_{56}H_{90}O_{19}Na^+$	1089.6016	1089.5992	2.11
$[M+Na\text{-ikem}]^+$	—	—	—	—	$C_{49}H_{78}O_{17}Na^+$	961.5103	961.5131	−2.91
$[M+Na\text{-cin}]^+$	$C_{49}H_{78}O_{17}Na^+$	961.5152	961.5131	2.18	—	—	—	—
Y_3	$C_{42}H_{66}O_{14}Na^+$	817.4359	817.4345	1.71	$C_{42}H_{66}O_{14}Na^+$	817.4334	817.4345	−1.35
Y_2	$C_{35}H_{54}O_{11}Na^+$	673.3570	673.3558	1.78	$C_{35}H_{54}O_{11}Na^+$	673.3549	673.3558	−1.34
B_3	$C_{21}H_{36}O_9Na^+$	455.2239	455.2252	−2.86	$C_{21}H_{36}O_9Na^+$	455.2230	455.2252	−4.83
B_2	$C_{14}H_{24}O_6Na^+$	311.1449	311.1465	−2.96	$C_{14}H_{24}O_6Na^+$	311.1449	311.1465	−2.96

Separation and identification of the pregnane glycosides in the roots of *C. auriculatum*

Optimal chromatographic conditions were obtained after running different mobile phases with a reversed-phase C_{18} column and with different fragmentation voltages. The best results were observed with the Zorbax RX-C_{18} column using a gradient elution program of acetonitrile/water. The representative UV chromatogram at 220 nm and total ion chromatogram (TIC) of the purified ethanolic extract of *C. auriculatum* roots are shown in Figs. 4(a) and 4(b), respectively. A total of ten major peaks were observed in Fig. 4 with retention times at 9.8, 12.2, 12.8, 17.5, 20.6, 22.1, 24.8, 27.9, 29.3 and 30.9 min, corresponding to Pg-1 to Pg-10. They were achieved by base-line separation within an acceptable 35 min. Mass measurement accuracy for molecular ions and subsequent product ion spectra, along with characteristic retention times, provided highly reliable identification for the target markers. Pg-1, 2, 3, 4, 5, 6, 7, 8, 9 and 10 were unequivocally identified as auriculoside IV, cynauricuoside C, cynauricuoside A, wilfoside C1G, cyna-

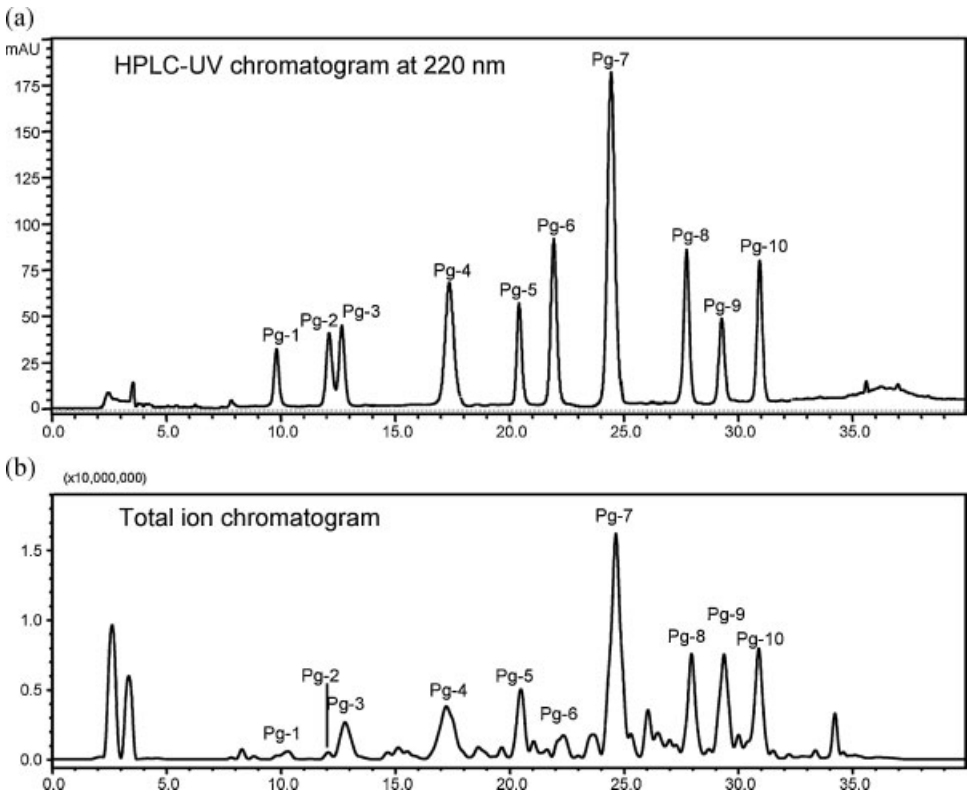

Figure 4. HPLC-UV chromatogram at 220 nm (a) and total ion chromatogram (b) of a purified ethanolic extract of *C. auriculatum*.

DOI: 10.1002/rcm

RCM

nauriculoside I, cynanauriculoside II, caudatin3-O-β-cym, wilfoside K1N, wilfoside C3N and wilfoside C1N, respectively, by comparison with reference compounds.

CONCLUSIONS

Ten pregnane glycosides from the roots of *C. auriculatum* have been firstly studied and characterized by ESI-IT-TOFMS. This approach was recommended to obtain the high mass accuracy measurement and best mass spectrometric structural information for these compounds, indicating that LC/ESI-IT-TOF/MS^n is a powerful analytical tool for the rapid characterization of pregnane glycosides. Our present investigation confirmed that MS/MS fragmentation pathways of the $[M+Na]^+$ ion provided valuable structural information about the glycosyl and aglycone moieties, opening perspectives for similar studies on other compounds. The pregnane glycosides in *C. auriculatum* could be divided into two major core groups, one with a caudatin skeleton characterized by loss of 128 Da corresponding to cinnamic acid at *C*-12, and the other with a kidjoranin skeleton characterized by loss of 148 Da representing ikemamic acid at *C*-12. A series of sugar-chain fragment ions such as the Y, B and A series provided valuable information for confirmation of the types of sugar compositions and the sequences of the sugar chain. Diagnostic ions and fragmentation pathways for pregnane glycosides proposed are useful for the identification of these compounds in natural products especially when reference compounds are lacking.

Acknowledgements

The authors greatly appreciate the financial support from the Key Program (No. 30530870) of the National Science Foundation of China, and National Key Technologies R&D Program of China.

REFERENCES

1. Li Y, Zhang J, Gu X, Peng Y, Huang W, Qian S. *Planta Med.* 2008; **74**: 551.
2. Shan L, Zhang WD, Zhang C, Liu RH, Su J, Zhou Y. *Phytother. Res.* 2005; **19**: 259.
3. Peng YR, Li YB, Liu XD, Zhang JF, Duan JA. *Phytomedicine* 2008; 10.1016/j.phymed.2008.02.021.
4. Ikeda T, Tsumagari H, Honbu T, Nohara T. *Biol. Pharm. Bull.* 2003; **26**: 1198.
5. Liu HW, Xiong ZL, Li FM, Qu GX, Kobayashi H, Yao XS. *Chem. Pharm. Bull.* 2003; **51**: 1089.
6. Yin J, Kouda K, Tezuka Y, Le TQ, Miyahara T, Chen YJ, Kadota S. *J. Nat. Prod.* 2003; **66**: 646.
7. Avula B, Wang YH, Pawar RS, Shukla YJ, Smillie TJ, Khan IA. *Rapid Commun. Mass Spectrom.* 2008; **22**: 2587.
8. Wang D, Liu Z, Guo M, Liu S. *J. Mass Spectrom.* 2004; **39**: 1356.
9. Schütz K, Kammerer DR, Carle R, Schieber A. *Rapid Commun. Mass Spectrom.* 2005; **19**: 179.
10. Guo H, Liu AH, Ye M, Yang M, Guo DA. *Rapid Commun. Mass Spectrom.* 2007; **21**: 715.
11. Ren L, Xue X, Zhang F, Wang Y, Liu Y, Li C, Liang X. *Rapid Commun. Mass Spectrom.* 2007; **21**: 3039.
12. Tai Y, Cao X, Li X, Pan Y. *Anal. Chim. Acta* 2006; **572**: 230.
13. Zheng Z, Zhang W, Kong L, Liang M, Li H, Lin M, Liu R, Zhang C. *Rapid Commun. Mass Spectrom.* 2007; **21**: 279.
14. Liu Y, Li J, Yu S, Abliz Z, Liu Y, Qu J, Liu J, Hu Y. *Anal. Chim. Acta* 2008; **611**: 187.
15. Yokosuka T, Yoshinari K, Kobayashi K, Ohtake A, Hirabayashi A, Hashimoto Y, Waki I, Takao T. *Rapid Commun. Mass Spectrom.* 2006; **20**: 2589.
16. Hao H, Cai N, Wang G, Xiang B, Liang Y, Xu X, Zhang H, Yang J, Zheng C, Wu L, Gong P, Wang W. *Anal. Chem.* 2008; **80**: 8187.
17. Ferrer I, Heine CE, Thurman EM. *Anal. Chem.* 2004; **76**: 1437.
18. Zhu ZY, Zhang H, Zhao L, Dong X, Li X, Chai YF, Zhang GQ. *Rapid Commun. Mass Spectrom.* 2007; **21**: 1855.
19. Tsukamoto S, Hayashi K, Mitsuhashi H. *Tetrahedron* 1985; **41**: 927.
20. Tsukamoto S, Hayashi K, Mitsuhashi H. *Chem. Pharm. Bull.* 1985; **33**: 2294.
21. Chen JJ, Zhang ZX, Zhou J. *Acta. Botan. Yunnan.* 1990; **12**: 197.
22. Wang YQ, Yan XZ, Gong SS, Fu WH. *Chin. Chem. Lett.* 2002; **13**: 543.
23. Domon B, Costello CE. *Glycoconjugate J.* 1988; **5**: 397.
24. Gu XJ, Yao N, Qian SH, Li YB, Li P. *Helv. Chim. Acta* 2009; **92**: 88.

DOI: 10.1002/rcm